

## Computational Molecular Modeling of Chitin and Chitosan

Nattida Rakapao<sup>1,2</sup> and Visit Vao-soongnern<sup>\*1,2</sup>

Laboratory of Computational and Applied Polymer Science<sup>1</sup>, School of Chemistry<sup>2</sup>,  
Institute of Science, Suranaree University of Technology, Nakhon Ratchasima, 30000

### Abstract

Molecular modeling has been performed at two different level structures of chitin and chitosan *i.e.* single chain conformation and amorphous phase. The results reported provide a detailed description of the low-energy conformers of the dimer segments and an insight into the disordered state of the polysaccharide chains. Deacetylation of chitin acetylamine groups by chemical reaction has a significant effect on the conformational properties of the glycosidic bonds linking two repeat units. Both the location and the relative energies of the low energy areas of the potential energy surfaces slightly differ. Consequently, the predicted unperturbed polymer chain extension strongly depends on the structure, The predicted characteristic ratio ( $C_\infty$ ) ranges from 32.8 for an idealized pure 0% NAc chitosan and 38.9 for a 100% acetylated pure chitin. The characteristic ratio ( $C_\infty$ ) is found to increase for a degree of acetylation between 0 and 60%; then no significant variation is observed above DA of 60%. The amorphous bulk model was then constructed to model the solid state of these polysaccharide. The estimated cohesive energy parameters reveal that inter-chain interactions are stronger for the chitosan chain than that for chitin.

### 1. Introduction

Chitin is one of the most abundant natural polysaccharide produced in the world; it is extracted from crab or shrimp shells. It consists of *N*-acetyl *D*-glucosamine repeat units connected by a  $\beta$ 1-4 linkage. The most important derivative is obtained by partial hydrolysis of the acetyl groups in alkaline conditions to obtain a copolymer based on *D*-glucosamine and *N*-acetyl *D*-glucosamine units. The physical properties of the polymers obtained depend on the average degree of acetylation (DA) and on the distribution of the acetyl groups along the chains. One of the most important property of chitosan is that it becomes soluble in acidic medium (due to the  $-\text{NH}_2$  group protonation in C-2 position) when the degree of acetylation is lower than a value around 0.5; but this limit depends essentially of the acetyl distribution: blockwise distribution chitosan is more difficult to solubilize in acid than for a random distribution of the acetyl. These elements make the characterization of these polymers difficult due to the lack of solubility and then to the presence of aggregates which disturbs molecular weight and intrinsic viscosity determinations. The lack of solubility originates from interchain interactions due to H-bonds or hydrophobic interactions depending on the structure of the polymer or create during purification and isolation of the polymer. It is the reason why it is important to be able to predict the different intrinsic characteristics of chitosan based on a molecular modeling analysis. In this respect, one determined the characteristic ratio  $C_\infty$  of chitin and chitosan to analyze the role of the acetyl groups on the local stiffness of these polymers.

## 2. Hierarchical levels of molecular modeling

### 2.1 Monomeric units and glycosidic linkages

As a general rule in the conformational analysis of carbohydrates, the global shape of a disaccharide is mainly governed by the rotations about the glycosidic linkages. The two disaccharides that represent the basic repeating units of chitin and chitosan are presented in Fig. 1. Chitin and chitosan represent the backbone with the acetlyamine (NHCOCH<sub>3</sub>) and amine (NH<sub>2</sub>) groups, respectively. Number of amine groups are represented as the degree of acetylation. The global shape of a disaccharide i.e. the relative orientation of a monosaccharide with respect to the other is strongly dependant on the torsion angles  $\Phi$  and  $\Psi$  across the glycosidic bonds:  $\phi = \text{O}-5'-\text{C}-1'-\text{O}-1'-\text{C}-4$ ;  $\psi = \text{C}-1'-\text{O}-1'-\text{C}-4-\text{C}-5$ . Conformational space is then systematically explored by stepping those torsion angles in regular increments (10°) over the whole angular range. For each conformational microstate, a geometry optimization is performed by allowing the Cartesian coordinates of each atom to vary except those defining the  $\Phi$  and  $\Psi$  torsion angles. Calculations are performed using AMBER force field whose special parameters for carbohydrates were added. The method to energy evaluations should correctly describes the conformational behavior of carbohydrates; in particular it should reproduce specific stereoelectronic effects such as anomeric and exoanomeric effects. The choice of dielectric constant is 78 allowing aqueous solutions to be modelled.

### 2.2. Random conformations of the chain

Assuming that the ring conformation of the monomer and the bridge angle is fixed, the glycoside structure is rigid, and it can be represented by a virtual bond  $\{l_i; i = 1, 2, \dots, n\}$  joining adjacent bridge-head oxygens. The mean-square end-to-end length of such a sequence is given by (the angular bracket denote averaging with respect to the Boltzmann distribution.)

$$\langle r_n^2 \rangle = \langle (\sum l_i) \cdot (\sum l_j) \rangle = \sum_{i=1}^n l_i^2 + 2 \sum_{i=1}^{n-1} \sum_{j=i+1}^n \langle l_i \cdot l_j \rangle$$

Establishing a rectangular coordinate system on each monomer so that the  $x$  coordinate lies along the virtual bond, and defining  $T_i$  as the matrix which transforms from the coordinate system  $(i+1)$  to the system  $(i)$  apart from the translation, the above product is given by

$$\langle l_i \cdot l_j \rangle = (l_i \ 0 \ 0) \langle T_i T_{i+1} \dots T_{j-1} \rangle (l_j \ 0 \ 0)$$

Assuming that under  $\theta$  conditions the energy of the polymer is approximately equal to the sum of the dimer energies, then to a good approximation

$$\langle T_i T_{i+1} \dots T_{j-1} \rangle = \prod_{k=i}^{j-1} \langle T_k \rangle$$

The matrix  $\langle T_k \rangle$  transforms from the coordinates of  $l_{k+1}$  to  $l_k$ , averaged assuming a Boltzmann distribution of the angles of rotation  $\phi, \psi$  about the glycosidic and aglycone bonds respectively, and the angle  $\chi$ , rotation about the C'<sub>5</sub>-C'<sub>6</sub> bond

$$\langle T_k \rangle = \frac{\int \int \int T(\phi, \psi) \exp(-E(\phi, \psi)/kT) d\phi d\psi}{\int \int \int \exp(-E(\phi, \psi)/kT) d\phi d\psi}$$

The characteristic ratio is given by the limit

$$C_\infty = \lim_{n \rightarrow \infty} C_n \quad \text{where } C_n = \langle r_n^2 \rangle / nl^2$$

and  $l$  is the root-mean-square virtual bond length. From Eq. 1, 2, and 3 it follows that

$$C_n = 1 + (2/n) (1 \ 0 \ 0) \sum_{i < j} \sum_k \prod_k \langle T_k \rangle (1 \ 0 \ 0)^T$$

For regular monomer sequences the summations can be carried out analytically, but for irregular sequences this expression is very inconvenient. However, Flory and Jernigan have shown that the characteristic ratio may be obtained as

$$C_n = 1 + (2/n) (1 \ 0 \ 0) \prod_i^{n-1} G_i (0 \ l \ 1)^T \quad \text{where} \quad G_i = \begin{pmatrix} 1 & l_i \langle T_i \rangle & 0 \\ 0 & \langle T_i \rangle & l_i \\ 0 & 0 & 1 \end{pmatrix}$$

$l_i^T$  is the transpose of  $l_i$  and  $\mathbf{0}$  is a null matrix of appropriate order. Using this formulation,  $C_n$  for a particular sequence of  $n$  monomers is obtained as an average over all conformations of that molecule by forming the appropriate product of  $G$  matrices.

### 2.3. Amorphous solids

The amorphous bulk of the polymer is modelled by periodic cubic microstructures. The first repeat unit is filled into the box by choosing place and orientation at random. Then, a random conformation of a polymer is built one residue at a time within the cell. As segments were added to the growing chain, the nonbond distances of the conformation generated were checked. We have used a unique chain of DP 50 and the initial density was set to 1.25 g/cm<sup>3</sup>. An amorphous ensemble containing five independent conformations is constructed. The generated structures are then equilibrated by performing energy relaxation. Minimizations were performed by both steepest descent and conjugated gradient methods; the convergence criteria used was a root-mean-square (rms) force less than 0.1 (kcal/mol)/Å for the polymer and 0.1 (kcal/mol)/Å<sup>3</sup> for the stresses on the periodic boxes. Both convergence criteria were simultaneously satisfied for the system to be relaxed completely.

### 3. Results and Discussion

#### 3.1. Flexibility of the glycosidic bonds: potential energy surfaces

The calculated adiabatic conformational energy surfaces ( $\phi$ ,  $\psi$ ) for isolated dimers of four disaccharides are presented as potential energy contour maps in Figure 1. The energies are given relative to the lowest minimum. Both the adiabatic energy surfaces and the slight difference in the geometrical parameters between the minima suggest a limited effect of the nature of the different substitutions on atom C-2 and C-2', for 1-4 linked  $\beta$ -D-glucopyranosides. All maps show a large potential well extended in the  $\Psi$  direction that encompasses the lowest energy minima. It corresponds to extended conformations near the twofold helix. Liberation motion within this surface seems easy for those four compounds. However, the total area covered by the upper contour shows dissimilarity between the four maps. It is larger for C3 and C4 and lower for C1 and C2. This suggests that the bulkiness of the acetamido group will affect the flexibility of the adjacent glycosidic bond toward the reducing end. There is a less pronounced effect when the substituent is located on the reducing unit; this is probably due to its spatial location, far from the glycosidic bond. It is expected that the DA together with the distribution of the monomeric units should have some influence on the predicted hydrodynamic parameters of the long chains.

#### 3.2. Conformational behavior of the polymer chains

From the potential energy surfaces of the parent disaccharides, normalized Boltzmann abundances of each conformational microstate at 300 K could be calculated. The method described in Section 2.2 was employed to calculate the average properties such as the mean square of the end-to-end distance of the chain, which in turn allows the computation such as the characteristic ratio ( $C_\infty$ ) of polymers. The estimated asymptotic limit of the characteristic ratio is 32.8 for chitosan and 38.9 for chitin, indicating that chitin favors a more extended conformation when compared to chitosan. To address the question of the effect of the degree of *N*-acetylation on chain dimensions, chains differing in the amount of *N*-acetyl groups (10, 20, ..., 90%) were generated assuming a random distribution of the substituents. The dependence of the  $C_\infty$  on DA of the chitosan and chitin chains is shown in Fig. 2. At low *N*-acetyl content, between 0 and 60%, the calculated characteristic ratios are sensitive to the *N*-acetyl group content and the values increase as the amount of *N*-acetylated residue increases. Then they are not significantly different for the range of *N*-acetylation between 60 and 100% for which the curve shows a plateau indicating that, in this range of acetylation, the chain extension is globally the same. To investigate how the monomeric distribution influences the chain properties, calculations have been performed for chain having 50% glucosamine and 50% *N*-acetylglucosamine residues with different patterns of monomeric distribution, random, alternate or in blocks.  $C_\infty$  of alternate AB copolymers increases by 15% whereas it decreases by only 2% for the  $A_2B_2$  ones when compared to the random (Bernouillian) chains. Furthermore, there is no significant variation of the characteristic ratio for copolymers having from 2 to 20 consecutive glucosamine and *N*-acetylglucosamine monomers. This suggests that the chain dimensions would be the same of samples having either a random or a block substitution pattern of the *N*-acetyl groups. In contrast, the alternate AB copolymer is stiffer when compared to the others.

### 3.3. Amorphous solids

The polymer in an amorphous bulk state is represented as an ensemble of cubic microscopic structures for which periodic continuation conditions are employed. As an initial step, the densities of simulated box were assumed to be  $1.0 \text{ g/cm}^3$  and we use these models to calculate the static and thermodynamic properties. The cohesive energy (CED) and Hildebrand's solubility ( $\delta$ ) parameter (the square root of the cohesive energy density) derived from the ensemble average of the intermolecular part of the internal energy per mole of substance are then calculated to check these amorphous models. The cohesive energy density is dependent on the chemical substitution of the polymer chains; the computed systems display a slight difference between chitin and chitosan. The values for chitin and chitosan are  $\delta = 20.16 \pm 0.29$  and  $21.03 \pm 0.69 \text{ (J/cm}^3)^{1/2}$ , respectively. The cohesive energy density is dependent on the chemical substitution of the polymer chains. It is expected that the amine groups of chitosan are involved in intermolecular interactions, and  $\delta$  values for the chitin polymer are relatively lower.

### 4. Conclusion

This work demonstrates that molecular modeling methods are able to predict with good confidence the behavior of polysaccharides in solution and in solid state phase. The role of the degree of substitution along the backbone and of the distribution of the side groups have been discussed. Substitution of acetylamine by amine groups has a considerable effect on the conformational properties of the chain. Condensed mechanically stable amorphous phases have also been generated. The predicted cohesive parameters show that chitosan is more stabilized by interchain interactions than that of the chitin. Some results of the present molecular modelling investigation are in accordance with both early theoretical approaches on related structures and by experimental measurements.

**Acknowledgement:** This work is supported by National Nanotechnology Center (Grant No. NN-B-22-m1-20-47-06)

### References

1. W.L. Mattice, U.W. Suter, *Conformational Theory of Large Molecules: The Rotational Isomeric State Model in Macromolecular Systems*, John Wiley & Sons, Inc.: New York, (1994)
2. D.A. Brant, K.D. Goebel, *Macromolecules*, 8, (1975), pp 522
3. K. Mazeau, C. Moine, P. Krausz, V. Gloaguen, *Carbohydrate Research*, 340, 18, (2005), pp 2752

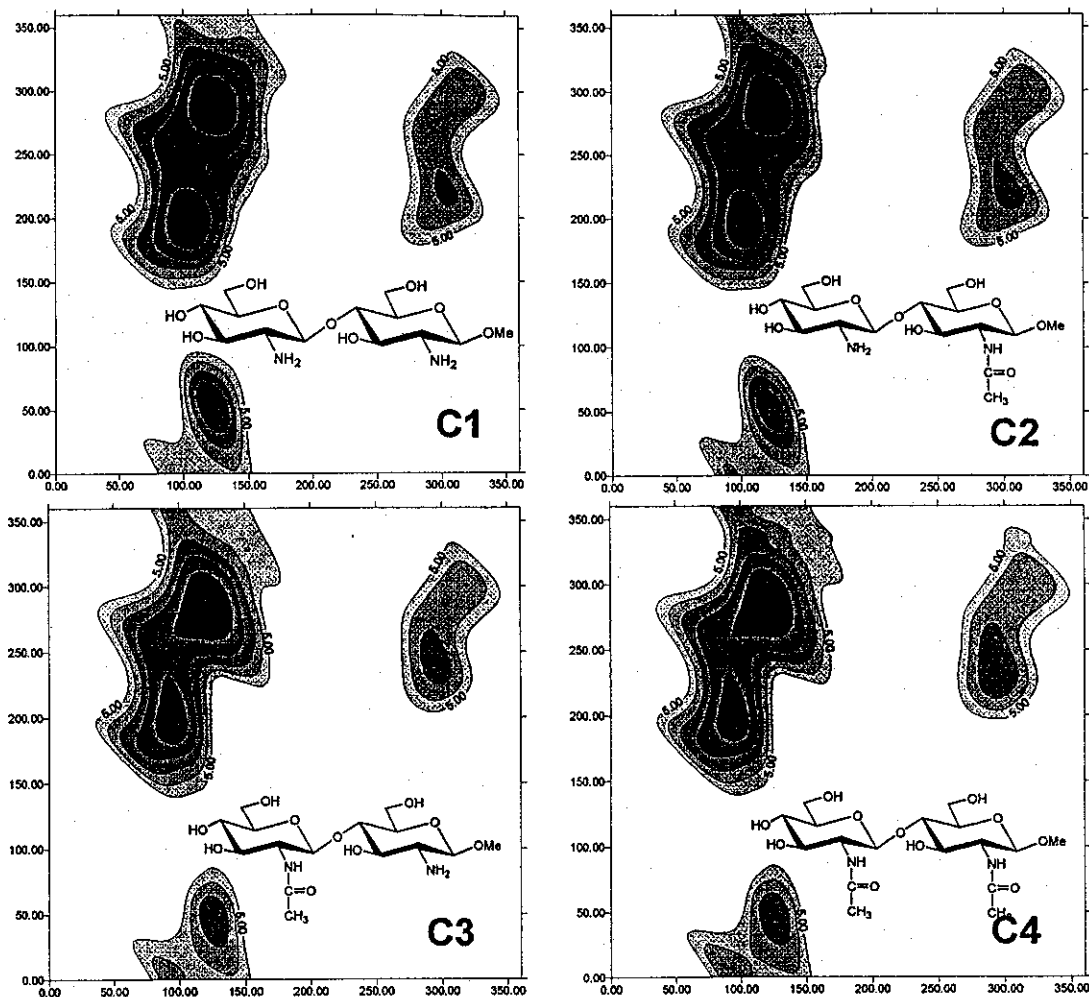


Fig. 1. The  $(\Phi, \Psi)$  potential energy surfaces of amine substituted dimer.

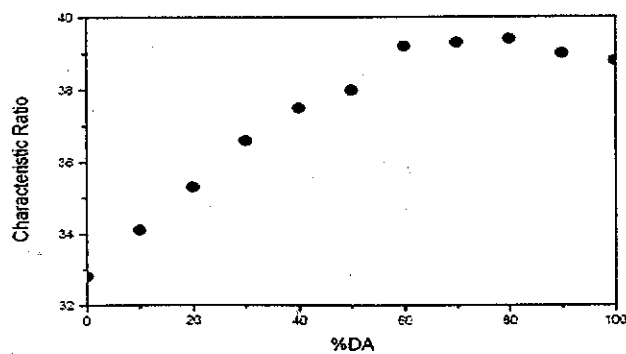


Fig. 2. Predicted influence of the *N*-Acetyl content in chitosan on the characteristic ratio